J. Fluid Mech. (1973), *vol.* 58, *part* 1, *pp.* 115–127
Printed in Great Britain

Two-dimensional bubbles in slow viscous flows. Part 2

By S. RICHARDSON
Applied Mathematics, University of Edinburgh

(Received 1 September 1972)

The present paper considers the behaviour of a two-dimensional inviscid bubble when placed in viscous fluid whose velocity at large distances varies parabolically, and whose motion is governed by the equations of Stokes flow. For arbitrary values of the surface tension at the bubble interface, this free boundary problem can be reduced to a coupled pair of transcendental equations.

When surface tension effects are large, the cross-section of the bubble is nearly circular. In the symmetric situation, with the bubble at the centre of a parabolic velocity profile, a reduction of the surface tension first produces a fattening at the rear of the bubble which then distorts further to form a re-entrant cavity. The solution also shows that the bubble moves faster than the undisturbed fluid velocity at its centre. When in an asymmetric position, the bubble has a drift velocity taking it towards the symmetric position.

1. Introduction

In an earlier paper (Richardson 1968, hereafter referred to as Part 1) complex-variable methods were used to examine some problems of two-dimensional Stokes flow involving free surfaces, with surface tension effects included. As an illustration, the behaviour of a two-dimensional inviscid bubble in (*a*) a shear flow, and (*b*) a pure straining motion was considered. It was shown that, in both cases, the bubble had an elliptical cross-section, the eccentricity and orientation of the ellipse being determined by a transcendental equation involving an elliptic integral.

The present paper considers the problem of a two-dimensional inviscid bubble placed in a parabolic flow. The methods used are those of Part 1. The cross-section is now no longer elliptical, but the problem reduces to the solution of a coupled pair of transcendental equations involving hyper-elliptic integrals. The interest of the present work lies in the results, rather than in the mathematical difficulties which motivated Part 1. Although the two-dimensional bubbles considered here might be thought to have little connexion with the three-dimensional bubbles encountered in practice, the solutions derived show remarkable similarities with the observed behaviour of the latter. Two observations in particular may be singled out: a large bubble moving under a pressure gradient through a circular tube shows the development of a re-entrant cavity at its rear end; small bubbles in flow down a circular tube tend to migrate towards the axis. Neither of these phenomena have, so far, been successfully explained, so that the fact that the

two-dimensional solutions show just this behaviour would seem to be worth recording.

We first recall some of the basic results from Part 1. A two-dimensional Stokes flow in the Cartesian x, y plane may be described in terms of two functions $\phi(z)$ and $\chi(z)$ of the complex variable $z = x+iy$, which are analytic within the flow domain. In terms of these, the velocity components (u, v) are given by

$$-v+iu = \phi(z)+z\overline{\phi'(z)}+\overline{\chi'(z)}, \tag{1.1}$$

while the vorticity ω and the pressure p are given by

$$\omega+ip/\mu = -4\phi'(z), \tag{1.2}$$

where μ is the viscosity, and an overbar is used to denote the complex conjugate.

For flows about bubbles, where there is no net force or couple on them and no source within them, both $\phi(z)$ and $\chi(z)$ are single-valued in the flow domain.

In the present case of a single bubble, the boundary conditions to be satisfied at its surface may be written as

$$\bar{z}\phi(z)+\chi(z) = 0 \tag{1.3}$$

and

$$\mathrm{Re}\left\{\frac{d\bar{z}}{ds}\phi(z)\right\} = \frac{T}{4\mu}, \tag{1.4}$$

where T is the surface tension and d/ds represents differentiation with respect to arc length along the free surface in a direction which leaves the bubble on the left. The pressure has here been taken to be zero within the bubble. These conditions then determine $\phi(z)$ and $\chi(z)$ uniquely.

2. Two-dimensional bubble at the centre of a parabolic flow

We first of all consider the symmetric situation illustrated in figure 1. The x axis is the line of symmetry in the direction of the basic flow and the flow is steady with respect to these axes. With the dominant parabolic flow at infinity given by $(u, v) \sim (-By^2, 0)$ we require

$$\left.\begin{aligned}\phi(z) &= \tfrac{1}{4}iBz^2-(ip_\infty/4\mu)z+O(1),\\ \chi(z) &= -\tfrac{1}{12}iBz^3+O(z),\end{aligned}\right\} \quad \text{as} \quad |z|\to\infty, \tag{2.1}$$

where p_∞ is the (unknown) pressure on $x = 0$ as $|y| \to \infty$, and there is a pressure gradient of magnitude $2B\mu$ driving this flow.

Proceeding as in Part 1, we map the flow domain onto the exterior of the unit circle in the ζ plane by $z = w(\zeta)$, where $w(\zeta)$ is analytic in $|\zeta| \geqslant 1$. This mapping is unique if we require $w(\zeta) \sim a\zeta$ as $|\zeta| \to \infty$, where a is a real constant. a is related to the bubble size and may be regarded as given: for large surface tension values, when the bubble has a circular cross-section, a is just the radius but, in general, it is not simply related to any geometrical property of the cross-section. As the other parameters vary, the same value of a will correspond to bubbles with different cross-sectional areas (see Part 1, § 5). We may choose the position of the origin in the z plane so that $w(\zeta) = a\zeta+O(1/\zeta)$ as $|\zeta| \to \infty$. The symmetry of the present problem implies

$$w(\zeta) = \overline{w(\bar{\zeta})}. \tag{2.2}$$

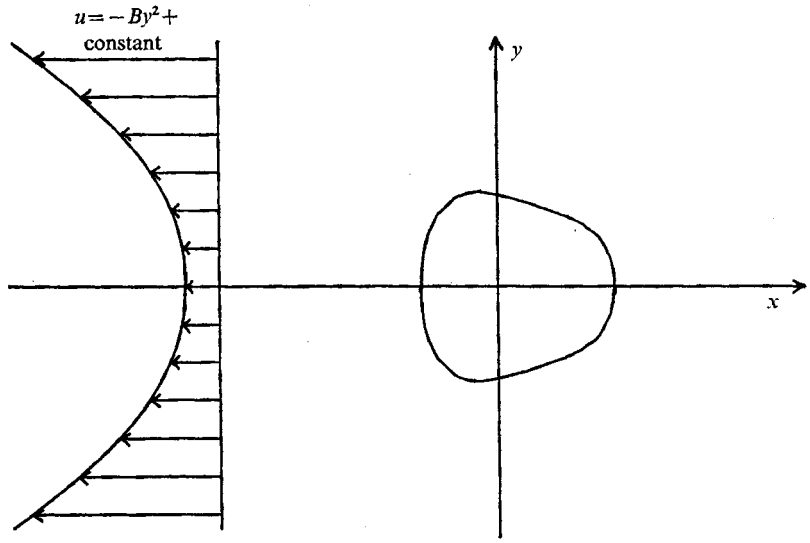

FIGURE 1. Co-ordinate system for the bubble at the centre of the parabolic flow.

If we define $\Phi(\zeta) = \phi(w(\zeta))$ and $\mathrm{X}(\zeta) = \chi(w(\zeta))$, these are both analytic functions of ζ in $|\zeta| \geqslant 1$, while

$$\left.\begin{aligned} \Phi(\zeta) &= \tfrac{1}{4}ia^2B\zeta^2 - (iap_\infty/4\mu)\zeta + O(1), \\ \mathrm{X}(\zeta) &= -\tfrac{1}{12}ia^3B\zeta^3 + O(\zeta), \end{aligned}\right\} \quad \text{as} \quad |\zeta| \to \infty. \tag{2.3}$$

The boundary conditions (1.3) and (1.4) on the bubble transform into two conditions to be satisfied on the unit circle $|\zeta| = 1$ (Γ, say), viz.

$$\overline{w(\zeta)}\,\Phi(\zeta) + \mathrm{X}(\zeta) = 0 \tag{2.4}$$

and

$$\mathrm{Re}\{i\zeta w'(\zeta)\,\overline{\Phi(\zeta)}\} = (T/4\mu)\,|w'(\zeta)|. \tag{2.5}$$

Condition (2.4) implies that the analytic continuation of $w(\zeta)$ into the interior of Γ is given by

$$w(\zeta) = -\overline{\mathrm{X}(1/\bar{\zeta})}/\overline{\Phi(1/\bar{\zeta})} \quad \text{for} \quad |\zeta| \leqslant 1, \tag{2.6}$$

and hence, using (2.3),

$$w(\zeta) \sim \frac{a}{3\zeta} + \frac{p_\infty}{3B\mu} \quad \text{as} \quad |\zeta| \to 0. \tag{2.7}$$

Apart from this simple pole at the origin, the only other possible singularities of $w(\zeta)$ are poles at points inside Γ which are inverse to zeros of $\Phi(\zeta)$.

As $T \to \infty$ we expect the bubble to have a circular section and $p_\infty \to -\infty$. It follows from (2.3) that we must then expect a zero of $\Phi(\zeta)$ within the flow field which approaches infinity. In fact, this simple limiting case may be solved by separating variables in the governing biharmonic equation. With $z = re^{i\theta}$ the result may be expressed in terms of a stream function ψ as

$$\psi(r, \theta) = -\tfrac{1}{3}B(r^3 - a^4/r)\sin^3\theta. \tag{2.8}$$

Translated into the present formalism, this yields a $\Phi(\zeta)$ which has just the one zero in the flow at infinity. We would therefore expect that, for general values of the surface tension, $\Phi(\zeta)$ has one, and only one, zero within the flow field. It then follows from (2.6) that $w(\zeta)$ must be of the form

$$w(\zeta) = a\left(\zeta + \frac{1}{3\zeta} + \frac{\beta}{\zeta - \alpha}\right), \quad \text{where} \quad \frac{\beta}{\alpha} = -\frac{p_\infty}{3B\mu a}, \tag{2.9}$$

and the zero of $\Phi(\zeta)$ is at $1/\bar{\alpha}$. In fact, in the present instance, (2.2) will imply that both α and β are real, while we must ensure that $|\alpha| < 1$, and that the four zeros of $w'(\zeta)$ are all in $|\zeta| < 1$.

As in Part 1, the other boundary condition (2.5) now allows $\Phi(\zeta)$ to be analytically continued into $|\zeta| < 1$. We then effect the decomposition

$$a/\{w'(\zeta)\overline{w'(1/\bar{\zeta})}\}^{\frac{1}{2}} = F_+(\zeta) + F_-(\zeta), \tag{2.10}$$

where $F_+(\zeta)$ is analytic in $|\zeta| \geqslant 1$ and vanishes at infinity, while $F_-(\zeta)$ is analytic in $|\zeta| \leqslant 1$, each being expressible as a contour integral involving the mapping function. This furnishes the functional relation, valid for all ζ,

$$\frac{\Phi(\zeta)}{\zeta w'(\zeta)} - \frac{Ti}{2\mu a}F_+(\zeta) = \frac{\zeta\overline{\Phi(1/\bar{\zeta})}}{\overline{w'(1/\bar{\zeta})}} + \frac{Ti}{2\mu a}F_-(\zeta). \tag{2.11}$$

But we know that the expression on the left-hand side is analytic in $|\zeta| \geqslant 1$ and tends to

$$\tfrac{1}{4}iaB(\zeta + 3\beta/\alpha) \quad \text{as} \quad |\zeta| \to \infty,$$

while the right-hand side is analytic in $|\zeta| \leqslant 1$, except for a pole at the origin, where it behaves as

$$-\frac{iaB}{4}\left(\frac{1}{\zeta} + \frac{3\beta}{\alpha}\right) + \frac{Ti}{2\mu a}F_-(0) + O(\zeta) \quad \text{as} \quad |\zeta| \to 0.$$

It thus follows, by Liouville's Theorem, that each side is equal to

$$\tfrac{1}{4}iBa(\zeta - 1/\zeta),$$

plus the same constant, so that

$$\frac{\Phi(\zeta)}{\zeta w'(\zeta)} = \frac{iaB}{4}\left(\zeta - \frac{1}{\zeta}\right) + \frac{3iaB}{4}\frac{\beta}{\alpha} + \frac{Ti}{2\mu a}F_+(\zeta) \tag{2.12}$$

and

$$3\beta = (T/a^2B\mu)\,\alpha F_-(0). \tag{2.13}$$

A further condition has now to be imposed, for $\Phi(\zeta)$ must have a zero at $1/\alpha$. Since $w'(\zeta)$ cannot have a zero there, this simply requires that the right-hand side of (2.12) vanishes at $\zeta = 1/\alpha$, or

$$\alpha^2 - 3\beta - 1 = (2T/a^2B\mu)\,\alpha F_+(1/\alpha). \tag{2.14}$$

The problem for given surface tension is thus reduced to the solution of the coupled pair of transcendental equations (2.13) and (2.14) for α and β. The mapping (2.9) then gives the bubble outline, while (2.12) and (2.6) furnish $\Phi(\zeta)$ and $\mathrm{X}(\zeta)$ to give a complete description of the flow.

At this stage it is instructive to consider the possibility of a solution at zero surface tension by putting $T = 0$ in (2.11). This evidently implies that β (and hence p_∞) vanishes, and leads to the solution

$$w(\zeta) = a(\zeta + 1/3\zeta), \tag{2.15}$$

$$\Phi(\zeta) = \frac{ia^2B}{4}\left(\zeta^2 - \frac{4}{3} + \frac{1}{3}\frac{1}{\zeta^2}\right), \tag{2.16}$$

$$\mathrm{X}(\zeta) = -\frac{ia^3B}{12}\left(\zeta^3 + \tfrac{5}{3}\zeta - \frac{11}{3}\frac{1}{\zeta} + \frac{1}{\zeta^3}\right). \tag{2.17}$$

Hence the bubble section is an ellipse with a semi-major axis of length $\frac{4}{3}a$ in the flow direction and a semi-minor axis of length $\frac{2}{3}a$. Transforming back to the z plane we find that, at large distances,

$$\phi(z) = \frac{iB}{4}z^2 - \frac{ia^2B}{2} + O\left(\frac{1}{z^2}\right),$$

$$\chi(z) = -\frac{iB}{12}z^3 - \frac{ia^2B}{18}z + O\left(\frac{1}{z}\right).$$

The first terms in $\phi(z)$ and $\chi(z)$ give the required dominant parabolic velocity profile. The constant term in $\phi(z)$ and the linear term in $\chi(z)$ give rise to an added constant velocity at infinity

$$u = -\tfrac{4}{9}a^2B. \tag{2.18}$$

This is a negative velocity in the x direction, and hence such a bubble placed at the centre of a parabolic velocity profile will move faster than the undisturbed fluid velocity at its centre. Evidently, the zero shear stress at the bubble's surface, and the pressure drop along its length, combine to give this excess velocity. Since the semi-minor axis has length $\frac{2}{3}a$, this excess velocity is just equal to the velocity difference in the undisturbed parabolic profile between the bubble's centre and its edge.

Returning to the general case we have, from (2.9),

$$w'(\zeta) = aP(\zeta)/\zeta^2(\zeta - \alpha)^2, \tag{2.19}$$

where

$$P(\zeta) = (\zeta^2 - \tfrac{1}{3})(\zeta - \alpha)^2 - \beta\zeta^2, \tag{2.20}$$

and $P(\zeta)$ is to have its four zeros in $|\zeta| < 1$. Thus the equations to be solved, (2.13) and (2.14), can be written, with $Z = T/a^2B\mu$, as

$$3\beta = Z\alpha G_1(\alpha, \beta) \tag{2.21}$$

and

$$\alpha^2 - 3\beta - 1 = 2Z\alpha^2 G_2(\alpha, \beta), \tag{2.22}$$

where

$$\left.\begin{aligned} G_1(\alpha,\beta) &= \frac{1}{2\pi i}\int_{\Gamma'} \frac{(t-\alpha)(1-\alpha t)\,dt}{t^2\{P(t)\,P(1/t)\}^{\frac{1}{2}}} = \frac{1}{\pi}\int_0^\pi \frac{(1 - 2\alpha\cos\theta + \alpha^2)\,d\theta}{|P(e^{i\theta})|} = F_-(0), \\ G_2(\alpha,\beta) &= \frac{1}{2\pi i}\int_{\Gamma'} \frac{(t-\alpha)\,dt}{t\{P(t)\,P(1/t)\}^{\frac{1}{2}}} = \frac{1}{\pi}\int_0^\pi \frac{(\cos\theta - \alpha)\,d\theta}{|P(e^{i\theta})|} = \frac{1}{\alpha}F_+\left(\frac{1}{\alpha}\right), \end{aligned}\right\} \tag{2.23}$$

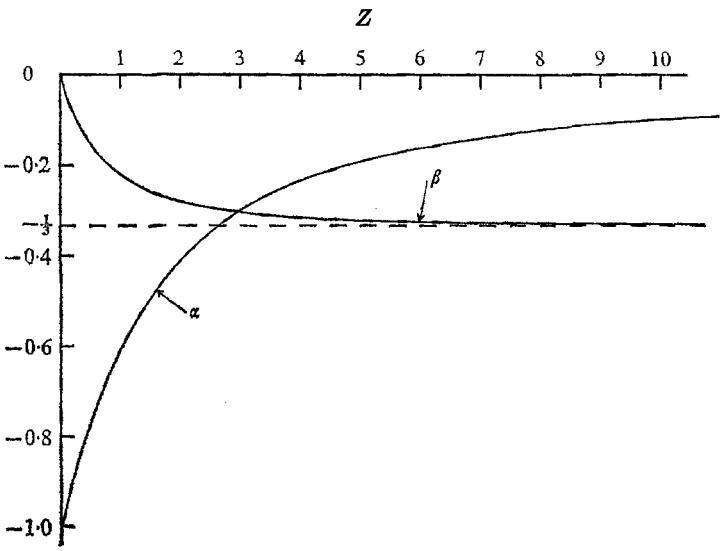

FIGURE 2. Variation of the real parameters α and β with Z for the bubble at the centre of the parabolic velocity profile.

Γ' being the unit circle in the t plane described anticlockwise. We thus have hyper-elliptic integrals involving the square root of polynomials of degree eight in the integrand, rather than the (tabulated) elliptic integrals obtained in Part 1.

If we add (2.21) and (2.22) there results

$$(1-\alpha^2)\{1+Z\alpha G_3(\alpha,\beta)\}=0, \tag{2.24}$$

where

$$G_3(\alpha,\beta)=\frac{1}{\pi}\int_0^{\pi}\frac{d\theta}{|P(e^{i\theta})|}. \tag{2.25}$$

It follows that the equations always have the solution $\alpha=\pm 1$, with β then given by (2.21), but this possibility must be discounted since we require $|\alpha|<1$.

Since both G_1 and G_3 are positive, it follows from (2.24) and (2.21) that both α and β (and hence p_∞) are negative for positive values of Z.

As $Z\to\infty$ we have $\alpha\to 0$ and $\beta\to-\frac{1}{3}$, so that the bubble section becomes the expected circle. For finite values of Z, equations (2.21) and (2.22) have been solved numerically for α and β, with $Z\geqslant 0{\cdot}09$. (Further details are given in Richardson 1967.) In fact, as $Z\to 0$, one can see that $\alpha\to-1$ and $\beta\to 0$, so that, in the limit, $P(\zeta)$ has two zeros on the integration contour, and this leads to numerical difficulties for values of Z below 0·1. Nevertheless, one can determine the variation of α and β with Z shown in figure 2.

Unfortunately, since $\alpha\to-1$ at the same time as $\beta\to 0$, it does *not* follow that the limiting solution as $Z\to 0$ is the same as that for $Z=0$ discussed earlier: the bubble section in the limit depends on the limit of the ratio $\beta/(1+\alpha)$. Only if this is zero is the result the elliptical section. In fact, the numerical work strongly suggests that this ratio tends to $-\frac{2}{3}$, but attempts to prove this analytically have failed. (In view of the difficulties encountered in the asymmetric situation discussed later, a rigorous proof ought not to assume the existence of a solution for small Z.) If we accept this value, the limiting section consists of the ellipse

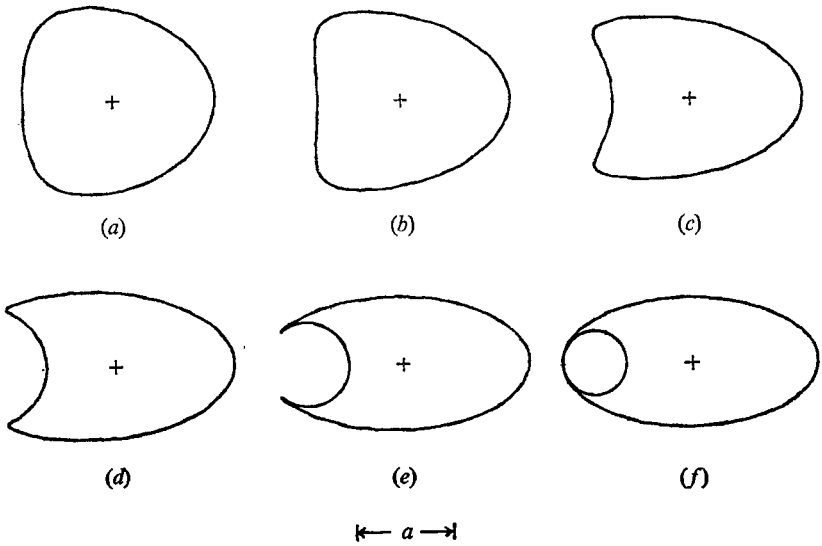

FIGURE 3. Bubble shapes at the centre of the parabolic velocity profile for varying Z.

	(*a*)	(*b*)	(*c*)	(*d*)	(*e*)	(*f*)
Z	4	2	1	0·5	0·1	0
α	−0·235	−0·409	−0·608	−0·772	−0·945	−1
β	−0·315	−0·279	−0·215	−0·145	−0·043	0

together with the circle of curvature at the rear of the ellipse with radius $\frac{1}{3}a$ and centre $(-a, 0)$. The viscous fluid occupies the exterior of the ellipse and the interior of the circle. Since the circle arises from an infinitesimally small region about $\zeta = -1$ in the ζ plane, there is no fluid motion within it. This is also evident physically, for the surface could not remain circular if motion were present. Since this fluid plays no part in the dynamics, the fact that the ellipse alone satisfies the limiting form of the equations is not surprising.

The bubble shapes given by the computed values of α and β for various values of Z, together with the above limiting shape for $Z = 0$, are shown in figure 3. The position of the origin of the z plane is marked by a cross, and the scale imposed by the value of a is also indicated. From these it can be seen how the bubble section deforms from its circular shape as Z decreases from infinity. An initial fattening at the rear, caused by the decrease of α from zero, develops into a re-entrant cavity at the rear which, for small values of Z, is approximately circular and joins the remainder of the bubble, which is approximately elliptical, by portions of very large, but finite, curvature. These portions arise from the two zeros of $w'(\zeta)$ which approach the unit circle. In the limit $Z \to 0$ proposed above, the cavity becomes totally enclosed and the large curvatures develop into cusps as they meet at the trailing edge.

An expansion for large $|z|$ reveals that, as well as the imposed parabolic velocity profile at infinity, there must also be a constant velocity given by

$$\frac{u}{a^2 B} = \frac{2Z}{3\pi}\int_0^{\pi} \frac{(1-2\alpha\cos\theta+\alpha^2)\cos\theta\, d\theta}{|P(e^{i\theta})|} - \frac{\beta}{4\alpha^2}(1+3\beta) - \tfrac{13}{12}\beta - \tfrac{4}{9}. \qquad (2.26)$$

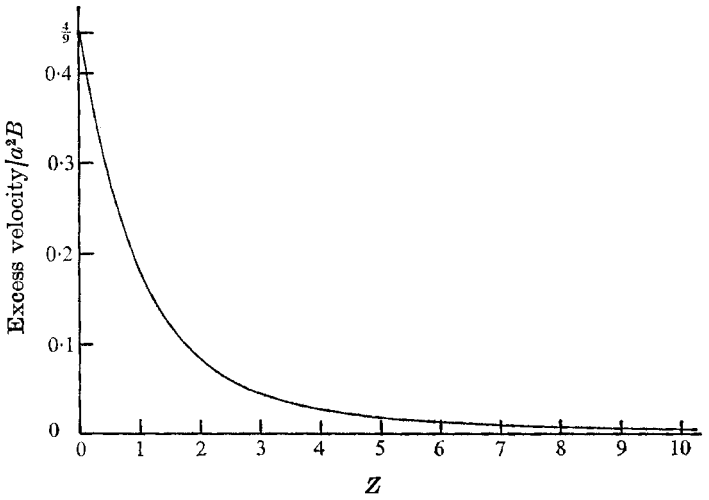

FIGURE 4. Variation of the excess bubble velocity with Z for the bubble at the centre of the parabolic profile.

This is always negative, so that the bubble moves faster than the fluid at its centre for all values of Z. The variation of this excess bubble velocity with Z is sketched in figure 4. For fixed a and B it is a maximum in the limit $Z \to 0$, when we recover (2.18): as Z increases the velocity decreases and tends to zero as $Z \to \infty$. In this limit, the section is a circle of radius a, and this contrasts with the behaviour of a solid circular cylinder which is free to move at the centre of a parabolic velocity profile. A simple calculation shows that such a cylinder of radius a moves slower than the undistributed fluid velocity at its centre by an amount $\frac{1}{2}a^2B$: there is a velocity defect, and the cylinder moves with a velocity which is the mean value of the basic flow velocity over the diameter perpendicular to the flow.

3. Two-dimensional bubble off-centre in a parabolic flow

Consider now the asymmetric situation illustrated in figure 5, where the bubble is placed a distance A from the centre of the parabolic profile. With the basic flow at infinity given by $(u, v) \sim (By(2A-y), 0)$ we require

$$\left.\begin{aligned} \phi(z) &= \tfrac{1}{4}iBz^2 + (\tfrac{1}{2}AB - ip_\infty/4\mu)z + O(1), \\ \chi(z) &= -\tfrac{1}{12}iBz^3 - \tfrac{1}{2}ABz^2 + O(z), \end{aligned}\right\} \quad \text{as} \quad |z| \to \infty. \tag{3.1}$$

The working is very similar to that of § 2, but the mapping $w(\zeta)$ now shows no symmetry. It may still be expected to have the form

$$w(\zeta) = a\left(\zeta + \frac{1}{3\zeta} + \frac{\beta}{\zeta - \alpha}\right), \tag{3.2}$$

but α and β will be complex. The analytic continuation of $w(\zeta)$ into the interior of the unit circle now yields

$$w(\zeta) \sim \frac{a}{3\zeta} + \frac{p_\infty}{3\mu B} + \tfrac{4}{3}Ai \quad \text{as} \quad |\zeta| \to 0, \tag{3.3}$$

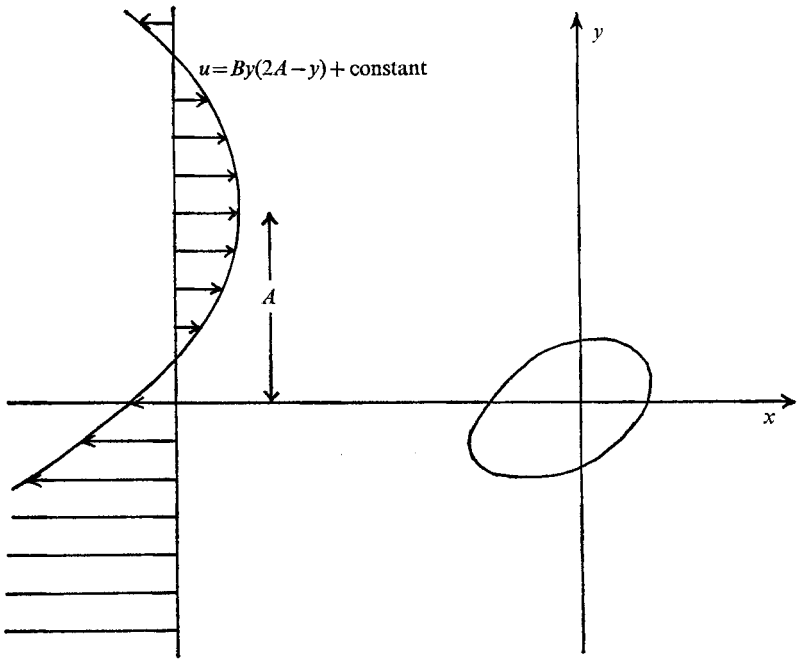

FIGURE 5. Co-ordinate system for the bubble off-centre in the parabolic flow.

so that, in this case,

$$\frac{\beta}{\alpha} = -\frac{p_\infty}{3\mu B} - \tfrac{4}{3}Ai, \tag{3.4}$$

and the imaginary part of β/α is fixed.

Since

$$\frac{\Phi(\zeta)}{\zeta w'(\zeta)} \sim \frac{iaB}{4}\zeta + \tfrac{3}{4}aBi\frac{\beta}{\alpha} - \frac{AB}{2} \quad \text{as} \quad |\zeta| \to \infty,$$

(2.12), (2.13) and (2.14) are replaced by

$$\frac{\Phi(\zeta)}{\zeta w'(\zeta)} = \frac{iaB}{4}\left(\zeta - \frac{1}{\zeta}\right) + \tfrac{3}{4}aBi\,\frac{\beta}{\alpha} - \frac{AB}{2} + \frac{Ti}{2\mu a}F_+(\zeta), \tag{3.5}$$

$$3\,\mathrm{Re}\{\beta/\alpha\} = (T/a^2B\mu)\,F_-(0), \tag{3.6}$$

$$\frac{iaB}{4}\left(\frac{1}{\bar{\alpha}} - \bar{\alpha}\right) + \tfrac{3}{4}aBi\frac{\beta}{\alpha} - \frac{AB}{2} + \frac{Ti}{2\mu a}F_+\left(\frac{1}{\bar{\alpha}}\right) = 0. \tag{3.7}$$

Equation (3.4) can be combined with (3.6) to give

$$\frac{3\beta}{\alpha} + 4\frac{A}{a}i = ZF_-(0), \tag{3.8}$$

while the identity (equation (3.19) of Part 1)

$$\overline{F_+(1/\bar{\zeta})} = F_-(\zeta) - F_-(0)$$

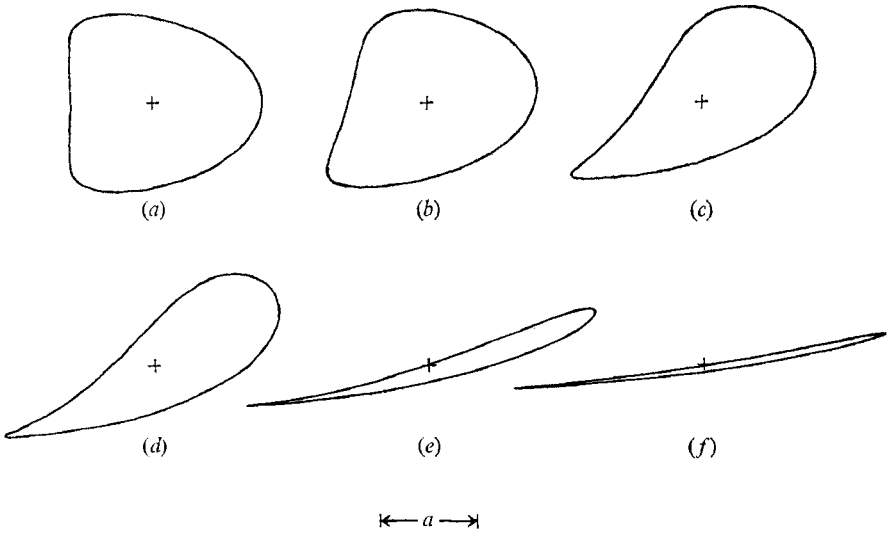

FIGURE 6. Bubble shapes off-centre in the parabolic velocity profile for varying A/a with $Z = 2$.

	(a)	(b)	(c)
A/a	0	0·2	0·6
α	$-0{\cdot}409$	$-0{\cdot}401+0{\cdot}043i$	$-0{\cdot}348+0{\cdot}112i$
β	$-0{\cdot}279$	$-0{\cdot}265+0{\cdot}137i$	$-0{\cdot}168+0{\cdot}361i$
	(d)	(e)	(f)
A/a	1	3	7
α	$-0{\cdot}276+0{\cdot}147i$	$-0{\cdot}078+0{\cdot}131i$	$-0{\cdot}020+0{\cdot}067i$
β	$-0{\cdot}033+0{\cdot}490i$	$0{\cdot}441+0{\cdot}454i$	$0{\cdot}594+0{\cdot}276i$

allows (3.6) and (3.7) to be combined as

$$\alpha-\frac{1}{\alpha}+\frac{3\beta}{\alpha}+\frac{2Ai}{a}=2ZF_{-}(\alpha), \tag{3.9}$$

where $Z = T/a^2B\mu$, as in § 2. For given values of Z and A/a, the coupled pair of equations (3.8) and (3.9) are to be solved for the complex parameters α and β. This can be done numerically and has been carried through for a number of fixed values of Z, for varying A/a. Further details and typical results may be found in Richardson (1967). The resulting variation in the bubble shape for $Z = 2$ is shown in figure 6.

For small values of Z there are again difficulties, as in the symmetric situation. For example, for $Z = 1$ it was possible to obtain sensible solutions for α and β only for $A/a \leqslant 0{\cdot}58$. The range of shapes for A/a up to this value is shown in figure 7 and it is evident that, for $A/a = 0{\cdot}58$, there is a zero of $w'(\zeta)$ very close to the unit circle, and it seems likely that larger values will push this zero onto the integration contour, when a solution will cease to exist. This conjecture is supported by the observation that an attempt to obtain a solution at zero surface tension, as was possible for $A = 0$, fails for $A \neq 0$. It is not clear, however, whether this breakdown occurs for all values of Z, if A/a is made large enough, or whether it is restricted to the smaller values. Experiments by Taylor (1934) and Rum-

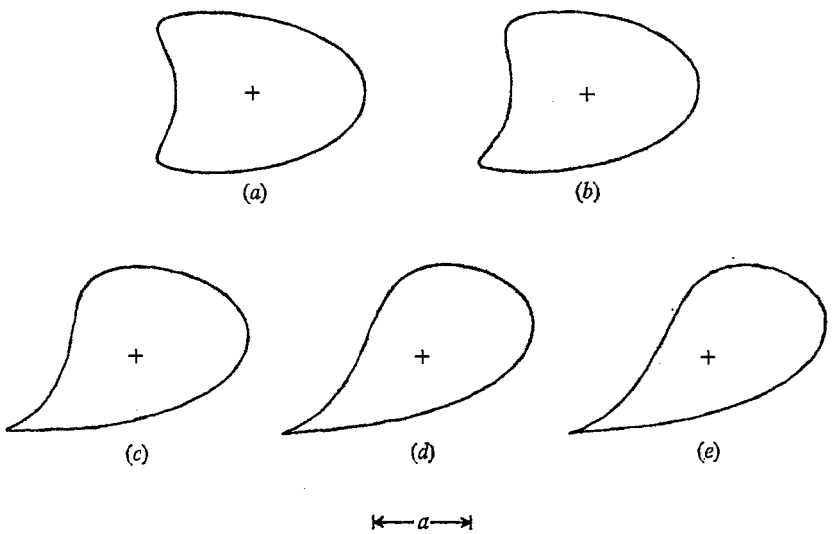

FIGURE 7. Bubble shapes off-centre in the parabolic velocity profile for varying A/a with $Z = 1$.

	(a)	(b)	(c)	(d)	(e)
A/a	0	0·1	0·3	0·5	0·58
α	$-0{\cdot}608$	$-0{\cdot}599+0{\cdot}019i$	$-0{\cdot}533+0{\cdot}051i$	$-0{\cdot}455+0{\cdot}079i$	$-0{\cdot}429+0{\cdot}089i$
β	$-0{\cdot}215$	$-0{\cdot}212+0{\cdot}086i$	$-0{\cdot}193+0{\cdot}234i$	$-0{\cdot}163+0{\cdot}340i$	$-0{\cdot}147+0{\cdot}376i$

scheidt & Mason (1961) show that a three-dimensional bubble placed in a shear flow tends to break up if the shear rate is too high. The results of Part 1 show that a solution for a two-dimensional bubble in a shear flow is possible for any shear rate, but these experimental observations suggest that one ought not to expect solutions to exist under all conditions.

As in the symmetric case, we can determine the behaviour at large distances and find that, as well as the parabolic velocity variation, we must impose a constant velocity, now given by

$$\frac{-v+iu}{a^2B} = \frac{aZ}{6\pi}\int_0^{2\pi} \frac{(2i\cos\theta - \sin\theta)\,d\theta}{|w'(e^{i\theta})|} - i\left\{\frac{\beta}{4\alpha^2}(1+3\beta)+\tfrac{3}{4}\beta+\tfrac{1}{3}\bar{\beta}+\tfrac{4}{9}\right\}+\frac{3}{2}\frac{A}{a}\frac{\beta}{\alpha}.$$

For A/a positive we find that both u and v are negative. The negative value of u once more implies that a bubble in a parabolic flow will move faster than the undisturbed fluid velocity at its centre, its centre being defined as the origin of the z plane which emerges from the transformation (3.2). The negative value of v is here of more interest for, in this low Reynolds number limit, a change of axes can be made, and this then implies that a bubble placed off-centre in a parabolic flow will drift, with velocity $-v$, towards the central position. This procedure involves the usual arguments to justify the application of the Stokes equations to a quasi-static situation (see Happel & Brenner 1965, p. 53, for example). The variation of this drift velocity with A/a for given Z is sketched in figure 8. A similar sketch for the excess velocity may be found in Richardson (1967).

As A/a becomes large one might expect the drift velocity to become small, since the flow approaches a shear flow more closely. However, this expectation

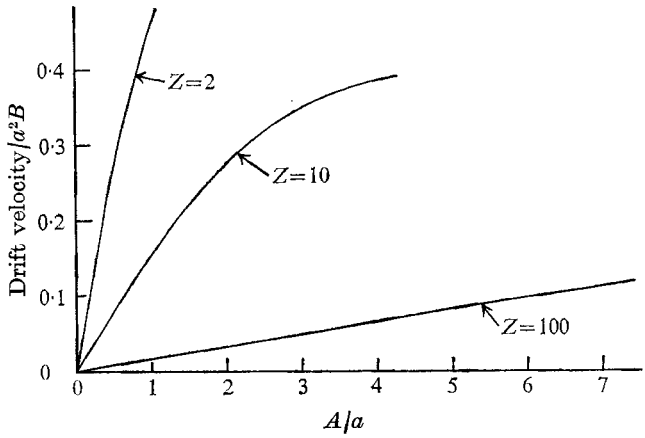

FIGURE 8. Variation of the drift velocity of the bubble towards the centre of the parabolic velocity profile with A/a, for given values of Z.

is not justified, for a parabolic profile $u = -By^2$ gives a local shear $k = -2By$ and a local rate of change of shear $dk/dy = -2B$. The drift velocity across the basic streamlines is evidently produced by a coupling between the shear and its rate of change, for it vanishes when the former vanishes at the centre, and also vanishes when the latter vanishes in a pure shear flow. Since neither of them vanish at large distances in a parabolic flow, this velocity should not be expected to approach zero there. Indeed, the numerical work suggests that the drift velocity increases with A/a in the range where a solution can be found, this being a natural consequence of a coupling between a rate of change of shear which remains constant and a shear which is increasing. In general, the behaviour of a deformable body in a flow field is more complex than might be expected from an analysis which regards it as being in a shear flow of the appropriate local strength, for this imposes a symmetry on the geometry which will not normally be present in practice.

4. Concluding remarks

As was noted in the introduction, the two-dimensional solutions obtained in the present paper show many features in common with the observed behaviour of three-dimensional bubbles. Two of these are, perhaps, worth mentioning in more detail.

Experiments by Cox (1963) and Goldsmith & Mason (1963) in which fairly large inviscid bubbles were introduced into a viscous fluid flowing through a circular tube show that the steady motion which ultimately results involves a bubble shape with a re-entrant cavity at the rear which is closely spherical, provided the surface tension is not too large. A photograph of such a bubble, taken from Cox (1963), is shown in figure 9 (plate 1). The bubble here is, of course, axially symmetric, but the lighting is such that we see its section in a plane through its axis. Moreover, the walls of the tube are obviously having a strong

effect on the motion. Nevertheless, the similarity with the two-dimensional solutions obtained here is rather striking.

Experiments with small bubbles introduced into a fluid flowing through a circular tube show that they migrate to the axis even at very low Reynolds numbers (Goldsmith & Mason 1962) in contrast to the behaviour of solid, neutrally buoyant spheres, which show a migration across the streamlines only at higher Reynolds numbers. Chaffey, Brenner & Mason (1965) consider this drift of the bubbles to be a wall effect, but it is evident that the curvature of the velocity profile alone, with the consequent asymmetry of the bubble outline, could also produce such a velocity.

The author is grateful to Dr B. G. Cox, of the University of Otago, Dunedin, New Zealand, for permission to reproduce the photograph of figure 9 from his dissertation. This thesis contains a large number of similar photographs which deserve a wider audience.

REFERENCES

CHAFFEY, C. E., BRENNER, H. & MASON, S. G. 1965 *Rheol. Acta*, **4**, 64. Correction in *Rheol. Acta* (1967), **6**, 100.

COX, B. G. 1963 Inviscid bubbles in viscous fluids. Ph.D. dissertation, University of Cambridge.

GOLDSMITH, H. L. & MASON, S. G. 1962 *J. Colloid Sci.* **17**, 448.

GOLDSMITH, H. L. & MASON, S. G. 1963 *J. Colloid Sci.* **18**, 237.

HAPPEL, J. & BRENNER, H. 1965 *Low Reynolds Number Hydrodynamics*. Prentice-Hall.

RICHARDSON, S. 1967 Slow viscous flows with free surfaces. Ph.D. dissertation, University of Cambridge.

RICHARDSON, S. 1968 *J. Fluid Mech.* **33**, 475.

RUMSCHEIDT, F. D. & MASON, S. G. 1961 *J. Colloid Sci.* **16**, 238.

TAYLOR, G. I. 1934 *Proc. Roy. Soc.* A **146**, 501.